VOLUME 73, NUMBER 18 JOC Featured Article September 19, 2008

Regiospecifically α-^{13}C-Labeled Porphyrins for Studies of Ground-State Hole Transfer in Multiporphyrin Arrays

Ana Z. Muresan,[†] Patchanita Thamyongkit,[†] James R. Diers,[‡] Dewey Holten,*[,§] Jonathan S. Lindsey,*[,†] and David F. Bocian*[,‡]

Department of Chemistry, North Carolina State University, Raleigh, North Carolina 27695-8204, Department of Chemistry, University of California, Riverside, California 92521-0403, and Department of Chemistry, Washington University, St. Louis, Missouri 63130-4889

jlindsey@ncsu.edu; david.bocian@ucr.edu; holten@wustl.edu

Received June 15, 2008

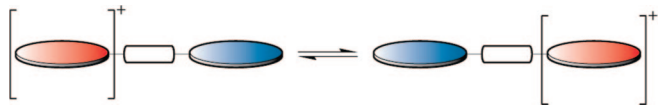

Insight into the electronic communication between the individual constituents of multicomponent molecular architectures is essential for the rational design of molecular electronic and/or photonic devices. To clock the ground-state hole/electron-transfer process in oxidized multiporphyrin architectures, a *p*-diphenylethyne-linked zinc porphyrin dyad was prepared wherein one porphyrin bears two ^{13}C atoms and the other porphyrin is unlabeled. The ^{13}C atoms are located at the 1- and 9-positions (α-carbons symmetrically disposed to the position of linker attachment), which are sites of electron/spin density in the a_{1u} HOMO of the porphyrin. The ^{13}C labels were introduced by reaction of KS^{13}CN with allyl bromide to give the allyl isothiocyanate, which upon Trofimov pyrrole synthesis followed by methylation gave 2-(methylthio)pyrrole-*2*-^{13}*C*. Reaction of the latter with paraformaldehyde followed by hydrodesulfurization gave dipyrromethane-*1,9*-^{13}*C*, which upon condensation with a dipyrromethane-1,9-dicarbinol bearing three pentafluorophenyl groups gave the tris(pentafluorophenyl)porphyrin bearing ^{13}C labels at the 1,9-positions and an unsubstituted meso (5-) position. Zinc insertion, bromination at the 5-position, and Suzuki coupling with an unlabeled porphyrin bearing a suitably functionalized diphenylethyne linker gave the regiospecifically labeled zinc porphyrin dyad. Examination of the monocation of the isotopically labeled dyad via electron paramagnetic resonance (EPR) spectroscopy (and comparison with the monocations of benchmark monomers, where hole transfer cannot occur) showed that the hole transfer between porphyrin constituents of the dyad is slow ($<10^6$ s^{-1}) on the EPR time scale at room temperature. The slow rate stems from the a_{1u} HOMO of the electron-deficient porphyrins, which has a node at the site of linker connection. In contrast, analogous dyads of electron-rich porphyrins (wherein the HOMO is a_{2u} and has a lobe at the site of linker connection) studied previously exhibit rates of hole transfer that are fast ($>5 \times 10^7$ s^{-1}) on the EPR time scale at room temperature.

Introduction

The rational design of molecular photonic and electronic devices composed of multiple constituents requires a deep understanding of the electronic interactions between the constituents.[1] For systems that undergo electrochemical oxidation as part of their functional properties, electronic communication can be probed by assessing the mobility of the holes formed

[†] North Carolina State University.
[‡] University of California.
[§] Washington University.

(1) Holten, D.; Bocian, D. F.; Lindsey, J. S. *Acc. Chem. Res.* **2002**, *35*, 57–69.

10.1021/jo8012836 CCC: $40.75 © 2008 American Chemical Society
Published on Web 08/22/2008

CHART 1

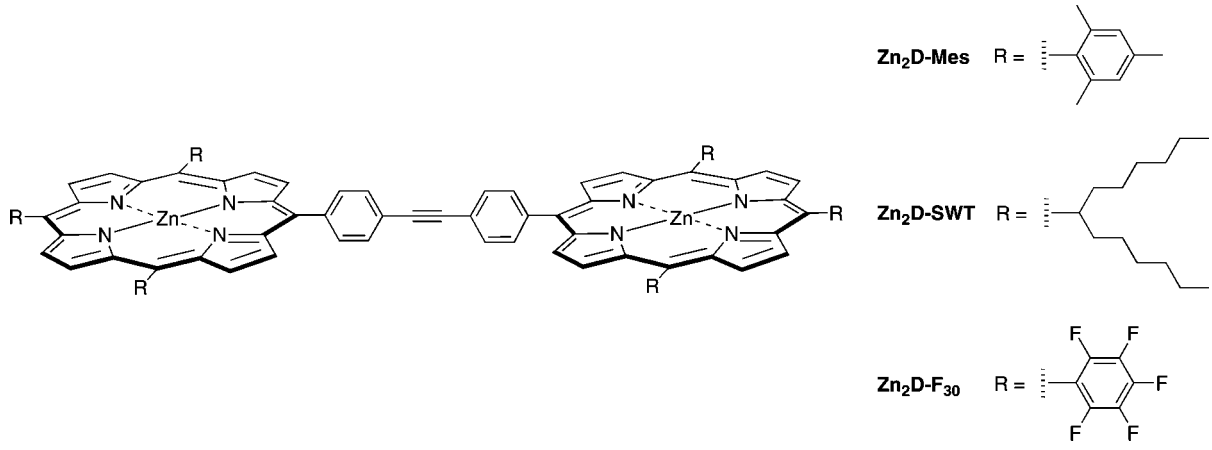

upon oxidation. Synthetic materials that undergo electrochemical oxidation at low potential and support the migration of the resulting holes can underpin a variety of novel molecular devices. One example is information storage with molecular materials, wherein information is stored in the discrete redox states of the molecules.[2] Another is efficient solar-energy conversion, which requires that holes generated after excited-state electron injection can move efficiently away from the anode, thereby preventing charge recombination.[3]

In synthetic light-harvesting antennas, studies of hole transfer have provided a basis for examining the extent of ground-state electronic communication among constituent pigments.[4] The studies of synthetic materials also provide a backdrop for analogous studies of natural systems. For example, chemical oxidation of natural photosynthetic light-harvesting proteins has yielded a single hole in the array of 32 bacteriochlorophyll molecules in the protein.[5−7] This hole then migrates among the large number of pigments. Magnetic resonance probing of the kinetics of hole migration yields information about the interactions among the pigments and how such interactions are influenced by changes in the matrix (liquid versus solid). Accordingly, a detailed understanding of hole migration may have important implications for the understanding of natural photosynthetic systems as well as artificial solar cells. Thus, understanding hole mobility in prototypical light-harvesting, charge-separation, and charge-storage systems is of fundamental interest.

To gain a deep understanding of hole mobility in molecular architectures, the ground-state hole-transfer characteristics of the monocations of several different types of tetrapyrrolic dyads have been investigated using EPR spectroscopy. The structures of the arrays are shown in Chart 1. All of the dyads are zinc chelates linked by a diphenylethyne group via the meso-positions of the macrocycle; the porphyrins differ only in the nature of the nonlinking meso substituents. One dyad contains mesityl substituents (**Zn_2D-Mes**),[8] one contains symmetrically branched tridecyl ("swallowtail") substituents (**Zn_2D-SWT**),[9] and the other contains pentafluorophenyl substituents (**Zn_2D-F_{30}**)[10] at these positions.

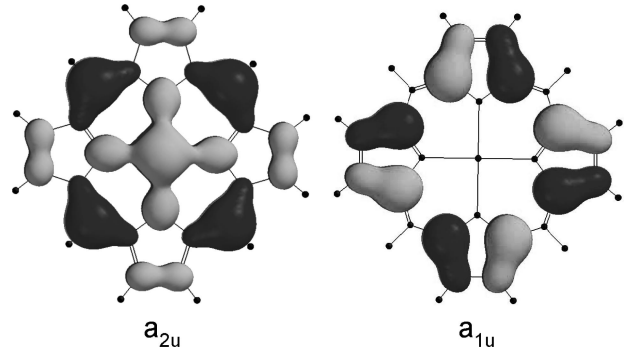

FIGURE 1. Metalloporphyrin a_{2u} and a_{1u} orbitals.

In the case of the monocations of the dyads with mesityl and swallowtail substituents, **[Zn_2D-Mes]$^+$** and **[Zn_2D-SWT]$^+$**, the hole resides in an a_{2u}-type HOMO and the ground electronic state is $^2A_{2u}$.[9,11] In this ground state, the electron (and spin) density resides primarily at the meso carbons and the pyrrole nitrogens (Figure 1).[12] Previous EPR studies of **[Zn_2D-Mes]$^+$** and **[Zn_2D-SWT]$^+$** have shown that the hole transfer between the two porphyrins is fast ($>10^7$ s^{-1}) on the time scale of the EPR experiment. The EPR time scale is determined by the nuclear hyperfine coupling between the unpaired electron and the ^{14}N nuclei of the pyrrole rings; this coupling is ~4.2 MHz.[11] The fast hole-transfer rates in the monocations of the dyads with $^2A_{2u}$ ground states are attributed to the fact that the linker that joins the two porphyrins is at a site of large electron/spin density.

In the case of the monocation of the dyad with pentafluorophenyl substituents, **[Zn_2D-F_{30}]$^+$**, the hole resides in an a_{1u}-type HOMO and the ground electronic state is $^2A_{1u}$.[10] In this ground state, the electron (and spin) density resides primarily

(2) Roth, K. M.; Dontha, N.; Dabke, R. B.; Gryko, D. T.; Clausen, C.; Lindsey, J. S.; Bocian, D. F.; Kuhr, W. G. *J. Vac. Sci. Technol. B.* **2000**, *18*, 2359–2364.
(3) Loewe, R. S.; Lammi, R. K.; Diers, J. R.; Kirmaier, C.; Bocian, D. F.; Holten, D.; Lindsey, J. S. *J. Mater. Chem.* **2002**, *12*, 1530–1552.
(4) del Rosario Benites, M.; Johnson, T. E.; Weghorn, S.; Yu, L.; Rao, P. D.; Diers, J. R.; Yang, S. I.; Kirmaier, C.; Bocian, D. F.; Holten, D.; Lindsey, J. S. *J. Mater. Chem.* **2002**, *12*, 65–80.
(5) Srivatsan, N.; Weber, S.; Kolbasov, D.; Norris, J. R. *J. Phys. Chem. B* **2003**, *107*, 2127–2138.
(6) Kolbasov, D.; Srivatsan, N.; Ponomarenko, N.; Jäger, M.; Norris, J. R., Jr. *J. Phys. Chem. B* **2003**, *107*, 2386–2393.
(7) Srivatsan, N.; Kolbasov, D.; Ponomarenko, N.; Weber, S.; Ostafin, A. E.; Norris, J. R., Jr. *J. Phys. Chem. B* **2003**, *107*, 7867–7876.
(8) Wagner, R. W.; Johnson, T. E.; Lindsey, J. S. *J. Am. Chem. Soc.* **1996**, *118*, 11166–11180.
(9) Thamyongkit, P.; Speckbacher, M.; Diers, J. R.; Kee, H. L.; Kirmaier, C.; Holten, D.; Bocian, D. F.; Lindsey, J. S. *J. Org. Chem.* **2004**, *69*, 3700–3710.
(10) Strachan, J.-P.; Gentemann, S.; Seth, J.; Kalsbeck, W. A.; Lindsey, J. S.; Holten, D.; Bocian, D. F. *J. Am. Chem. Soc.* **1997**, *119*, 11191–11201.
(11) Seth, J.; Palaniappan, V.; Wagner, R. W.; Johnson, T. E.; Lindsey, J. S.; Bocian, D. F. *J. Am. Chem. Soc.* **1996**, *118*, 11194–11207.
(12) Fajer, J.; Davis, M. S. In *The Porphyrins*; Dolphin, D., Ed.; Academic Press: New York, 1979; Vol. 4, pp 197−256.

CHART 2

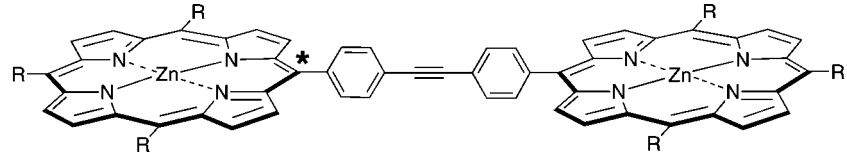

Zn_2D-Mes(5-^{13}C) (R = mesityl)
Zn_2D-SWT(5-^{13}C) (R = tridec-7-yl)

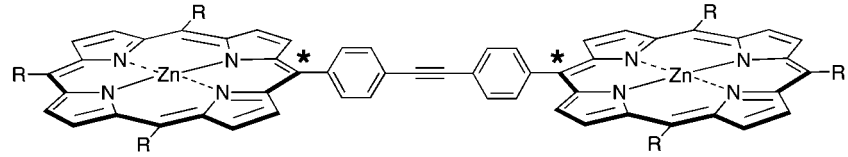

Zn_2D-Mes(5,5′-^{13}C) (R = mesityl)
Zn_2D-SWT(5,5′-^{13}C) (R = tridec-7-yl)

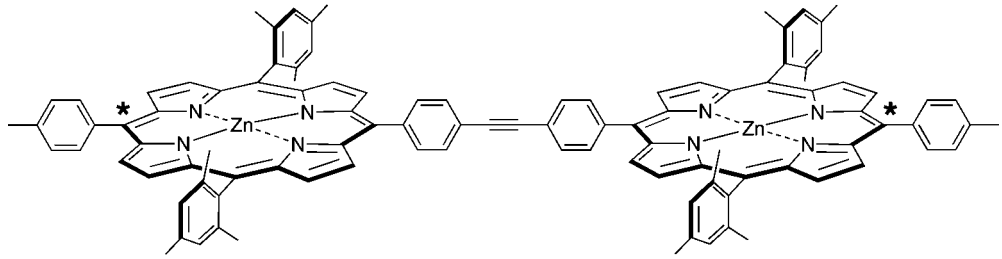

Zn_2D-Mes/T(15,15′-^{13}C)

at the α- and β-positions of the pyrrole rings; negligible spin density resides at the pyrrole nitrogen atoms (Figure 1).[12] The absence of ^{14}N nuclear hyperfine coupling in **[Zn_2D-F_{30}]**$^+$ renders these nuclei unsuitable as a hyperfine clock for assessing the hole-transfer characteristics. For this reason, our prior studies of hole transfer in **[Zn_2D-F_{30}]**$^+$ relied on the assessment of the hyperfine coupling to the ^{1}H nuclei at the β-pyrrole positions.[10] These studies suggested that hole transfer in **[Zn_2D-F_{30}]**$^+$ was slow ($<10^6$ s^{-1}) on the EPR time scale; however, this conclusion was tentative because the ^{1}H hyperfine couplings are not resolved and appear to be relatively small.

One approach for utilizing the EPR spectral features for assessing the hole-transfer characteristics in **[Zn_2D-F_{30}]**$^+$ and other types of dyads with $^1A_{1u}$ ground states is to incorporate a suitable isotopic label at a site of large electron/spin density. In this regard, we have previously used meso-^{13}C labeling to refine the time scale of hole transfer in monocations of porphyrin dyads with $^2A_{2u}$ ground states.[13] In these dyads, the hyperfine coupling between the unpaired electron and the meso-^{13}C nuclei is ∼16 MHz, which provides a hyperfine clock that is approximately 4 times faster than that of the ^{14}N nuclei. The various meso-^{13}C-labeled dyads that have been previously prepared are shown in Chart 2. In one set of dyads, one porphyrin incorporates a ^{13}C atom (*) at the meso-position to which the diphenylethyne linker is attached (**Zn_2D-Mes(5-^{13}C)**, **Zn_2D-SWT(5-^{13}C)**). In a second set of porphyrins, each porphyrin incorporates a ^{13}C atom (*) at the meso-position to which the diphenylethyne linker is attached (**Zn_2D-Mes(5,5′-^{13}C)**, **Zn_2D-SWT(5,5′-^{13}C)**). In a third type of dyad (**Zn_2D-Mes/T(15,15′-^{13}C)**), each porphyrin incorporates a ^{13}C atom (*) at the meso-position distal to the site of linker attachment. The EPR studies of the monocations of the five isotopically labeled dyads shown in Chart 2 revealed that hole-transfer is fast ($>4 \times 10^7$ s^{-1}) on the time scale of the meso-^{13}C hyperfine clock.[13]

In this paper, we implement the ^{13}C-labeling approach in a new synthetic design strategy that affords a definitive assessment of the hole-transfer characteristics of the $^2A_{1u}$ monocation **[Zn_2D-F_{30}]**$^+$. In the isotopically labeled dyad, ^{13}C atoms are incorporated at specific α-pyrrole positions, which are the sites of highest electron/spin density (Figure 1). The two dyads that have been synthesized are shown in Chart 3. The two dyads differ only in the presence of natural abundance H atoms at all nonsubstituted sites in the porphyrins and linker of **Zn_2D-F_{30}(1,9-^{13}C)** versus per deuteriation of all such sites in **Zn_2D-F_{30}(1,9-^{13}C)d_{24}**. The preparation of the dyads is accompanied by a series of porphyrin monomers that incorporate α-pyrrole-^{13}C, β-pyrrole-^{2}H, meso-carbon-^{2}H, and/or a combination of the various types of isotopic labels. The examination of the deuteriated molecules allows a definitive assessment of the magnitude of ^{1}H hyperfine coupling and whether this coupling is in fact reliable as a hyperfine clock for assessing the hole-transfer characteristics in dyads such as **[Zn_2D-F_{30}]**$^+$, which exhibit $^2A_{1u}$ ground states.

Gaining access to regiospecifically α-^{13}C-labeled porphyrins and dyads required considerable synthetic development. While

(13) Thamyongkit, P.; Muresan, A. Z.; Diers, J. R.; Holten, D.; Bocian, D. F.; Lindsey, J. S. *J. Org. Chem.* **2007**, *72*, 5207–5217.

(14) (a) Jordan, P. M. In *Biosynthesis of Heme and Chlorophylls*; Dailey, H. A., Ed.; McGraw-Hill, Inc.: New York, 1990; pp 55−121. (b) Battersby, A. R.; Leeper, F. J. *Chem. Rev.* **1990**, *90*, 1261–1274. (c) Scott, A. I. *Acc. Chem. Res.* **1978**, *11*, 29–36. (d) Shrestha-Dawadi, P. B.; Lugtenburg, J. *Eur. J. Org. Chem.* **2003**, 4654–4663. (e) Rivera, M.; Caignan, G. A. *Anal. Bioanal. Chem.* **2004**, *378*, 1464–1483.

CHART 3

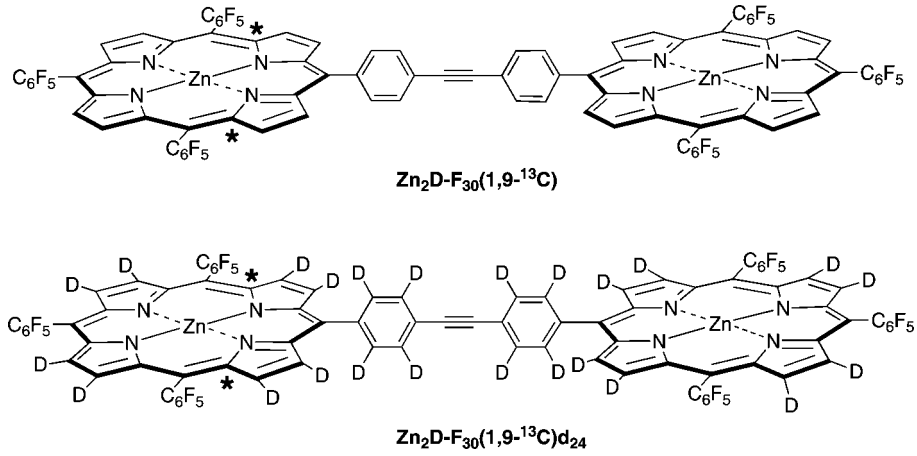

Zn_2D-F_{30}(1,9-^{13}C)

Zn_2D-F_{30}(1,9-^{13}C)d_{24}

CHART 4

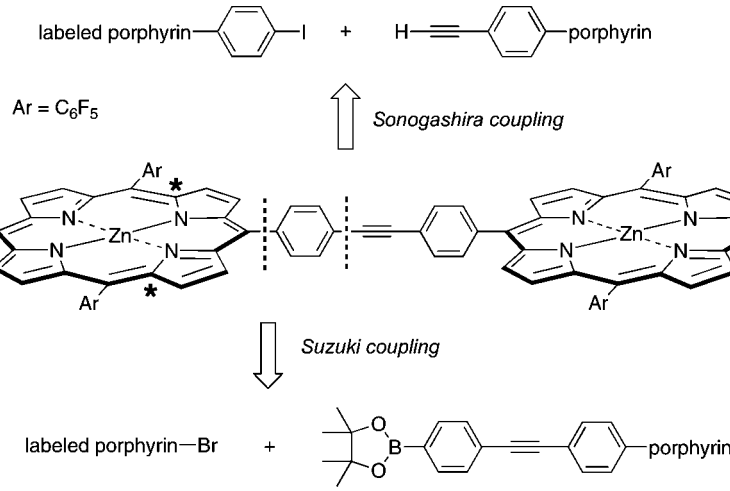

a number of ^{13}C-containing isotopologues of naturally occurring porphyrins have been prepared biosynthetically,[14] most synthetic porphyrins that bear ^{13}C labels contain the label at the meso-positions.[13] The dearth of α- (or β-) ^{13}C-labeled synthetic porphyrins[15] stems from the requirement to incorporate the ^{13}C label very early in a lengthy synthesis, namely in precursors to the pyrrole, whereas meso-^{13}C labels can be incorporated via readily accessible ^{13}C-labeled aldehyde or acyl units that are reacted with pyrrole (or pyrrole-containing units such as dipyrromethanes) in a late step of the porphyrin synthesis. Indeed, to our knowledge, no prior syntheses have placed ^{13}C labels at two distinct α-positions of a tetrapyrrole macrocycle. Collectively, the synthetic strategy described herein and the EPR studies of **[Zn_2D-F_{30}(1,9-^{13}C)]$^+$** and analogues provide new insight into the hole-transfer characteristics of the $^2A_{1u}$ monocations.

Results

I. Synthesis. 1. Strategy. Each target architecture (**Zn_2D-F_{30}(1,9-^{13}C)**, **Zn_2D-F_{30}(1,9-^{13}C)d_{24}**) shown in Chart 3 is unsymmetrical owing to the presence of distinct porphyrins attached to the diphenylethyne linker. The two porphyrins in each dyad differ only in the presence or absence of ^{13}C labels in the macrocycle. The preparation of such architectures requires a directed rather than statistical approach for coupling the two porphyrins. A synthetic strategy that has been widely used to prepare analogous compounds (e.g., wherein the two porphyrins differ only in the metalation state) entails the use of a Sonogashira coupling of two porphyrin building blocks (Chart 4).[8,16] In the Sonogashira approach, an iodophenylporphyrin and an ethynylphenylporphyrin are joined to create the diphenylethyne linker. The synthesis of the two A_3B-porphyrin building blocks was envisaged via an established "2 + 2" dipyrromethane + dipyrromethanedicarbinol approach,[17,18] wherein the isotopic labels in one of the porphyrins would be introduced via the dipyrromethane moiety. For the labeled dipyrromethane, we planned to take advantage of a recent stoichiometric synthesis of α,α′-bis(alkylthio)dipyrromethanes,[19] which upon use of a ^{13}C-labeled α-(alkylthio)pyrrole precursor would afford the requisite regiocontrol over the isotopic label. The desired ^{13}C-labeled dipyrromethane bearing a *meso*-(4-iodophenyl) group and α,α′-bis(methylthio) groups was prepared, but attempts to

(15) (a) Mispelter, J.; Momenteau, M.; Lhoste, J.-M. *J. Chem. Soc., Dalton Trans.* **1981**, 1729–1734. (b) Hu, S.; Mukherjee, A.; Piffat, C.; Mak, R. S. W.; Li, X.-Y.; Spiro, T. G. *Biospectroscopy* **1995**, *1*, 395–412. (c) Calle, C.; Schweiger, A.; Mitrikas, G. *Inorg. Chem.* **2007**, *46*, 1847–1855.

(16) Wagner, R. W.; Johnson, T. E.; Li, F.; Lindsey, J. S. *J. Org. Chem.* **1995**, *60*, 5266–5273.

(17) Rao, P. D.; Dhanalekshmi, S.; Littler, B. J.; Lindsey, J. S. *J. Org. Chem.* **2000**, *65*, 7323–7344.

(18) Zaidi, S. H. H.; Fico, R. M., Jr.; Lindsey, J. S. *Org. Process Res. Dev.* **2006**, *10*, 118–134.

(19) Thamyongkit, P.; Bhise, A. D.; Taniguchi, M.; Lindsey, J. S. *J. Org. Chem.* **2006**, *71*, 903–910.

remove the methylthio groups resulted in concomitant deiodination (vide infra). Hence, the Sonogashira route was abandoned.

A second strategy was pursued wherein a Suzuki coupling reaction is employed to join the labeled porphyrin and the unlabeled porphyrin bearing a diphenylethyne substituent. While more laborious, this route circumvented the limitations associated with removal of the methylthio groups that were encountered in the Sonogashira route. Suzuki couplings have been used to prepare a variety of porphyrin dyads, although heretofore most such dyads contained phenylene linkers rather than diphenylethyne linkers.[20] Other strategies for preparing porphyrin dyads have been investigated.[21]

Initially, we envisaged using a building block approach to prepare an analogue of **Zn_2D-F_{30}(1,9-^{13}C)** wherein all β-pyrrole protons were replaced with deuterium. The preparation of deuteriated building blocks with retention of the deuterium during the various synthetic procedures proved difficult. Ultimately, we found that dyad **Zn_2D-F_{30}(1,9-^{13}C)** could be converted to dyad **Zn_2D-F_{30}(1,9-^{13}C)d_{24}** by global deuteriation wherein not only the β-pyrrole protons but also the protons of the diphenylethyne linker were replaced with deuterium. The presence of deuterium on the diphenylethyne linker was not deleterious to the processes under investigation.

2. Labeled Porphyrin Monomers. The synthesis of a dipyrromethane bearing ^{13}C labels at the 1- and 9-positions cannot rely on the traditional one-flask condensation[22] of an aldehyde with excess pyrrole. Such a reaction with an α-^{13}C-labeled pyrrole would lead to a mixture of products wherein the labels would be located at the 1,9-, 1,6-, and 4,6-positions. Moreover, the one-flask condensation requires a large excess of pyrrole (20−100 molar equiv) to suppress the self-oligomerization and polymerization of the pyrrole−carbinol intermediate, which for a ^{13}C-containing pyrrole would be prohibitively expensive. The recent synthesis[19] of dipyrromethanes by condensation of stoichiometric quantities of α-(methylthio)-pyrrole and an aldehyde followed by removal of the α-methylthio groups appeared as a reasonable solution. The precursor to the α-(methylthio)pyrrole is an isotopologue of allyl isothiocyanate (mustard oil),[23] which can be prepared from allyl bromide and potassium thiocyanate[24] (Scheme 1).

Treatment of allyl bromide with KS^{13}CN at 55 °C gave the allyl thiocyanate, which isomerized to allyl isothiocyanate **1**. The isomerization of alkyl thiocyanates to alkyl isothiocyanates has been known since 1875. The reaction is lengthy (3 days); nevertheless, the product formed in high yield (86%) in a one-flask process, and no side products were observed except a trace of allyl thiocyanate (1% according to ^{1}H NMR and GC−MS analyses). Given the volatile nature of **1**, the crude product (99% purity as determined by ^{1}H NMR and GC−MS analysis) was carried forward to the next step. Following Trofimov pyrrole synthesis,[26] isothiocyanate **1** underwent deprotonation with KN(*i*-Pr)$_2$/*t*-BuOLi (generated in situ) followed by intramolecular cyclization. Subsequent treatment with water protonated selectively the nitrogen, and alkylation with methyl iodide afforded the isotopically labeled 2-(methylthio)pyrrole **2** in 56% yield.

SCHEME 1

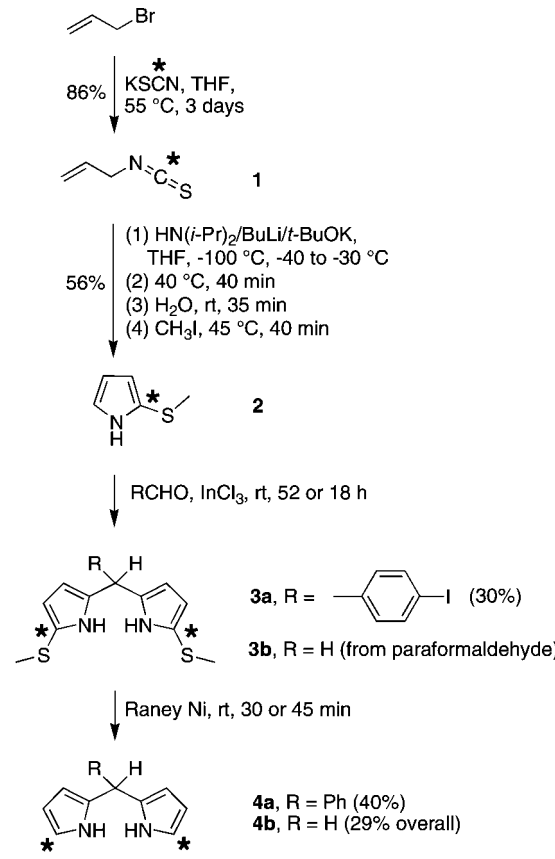

With the isotopically labeled 2-(methylthio)pyrrole **2** in hand, the synthesis of 1,9-bis(methylthio)dipyrromethanes bearing ^{13}C labels at the α-positions is thus possible. The condensation of **2** and 4-iodobenzaldehyde was carried out with a catalytic amount of $InCl_3$ at room temperature in the absence of any solvent. The reaction was monitored by TLC, and after 52 h, dipyrromethane **3a** was obtained in 30% yield. A similar reaction with paraformaldehyde afforded dipyrromethane **3b**, which was used in crude form in the subsequent reaction. The presence of the ^{13}C atom at the α-position of the methylthiopyrrole **2** and the 1,9-bis(methylthio)dipyrromethanes **3a**,**b** was clearly displayed by ^{1}H NMR spectroscopy, where the protons of the methyl group resonated as a doublet (J = 4.8 Hz) owing to coupling with the ^{13}C label.

The methylthio protecting groups of dipyrromethanes **3a**,**b** were cleaved by hydrodesulfurization using excess Raney Ni in a slurry at ambient conditions.[19] The desulfurization reaction requires use of at least a stoichiometric quantity of Raney Ni.[19,27] With iodophenyldipyrromethane **3a**, the reaction gave dipyrromethane **4a** wherein the two methylthio groups and the iodo

(20) Yu, L.; Lindsey, J. S. *Tetrahedron* **2001**, *57*, 9285–9298.

(21) Thamyongkit, P.; Yu, L.; Padmaja, K.; Jiao, J.; Bocian, D. F.; Lindsey, J. S. *J. Org. Chem.* **2006**, *71*, 1156–1171.

(22) Laha, J. K.; Dhanalekshmi, S.; Taniguchi, M.; Ambroise, A.; Lindsey, J. S. *Org. Process Res. Dev.* **2003**, *7*, 799–812.

(23) Remaud, G. S.; Martin, Y.-L.; Martin, G. G.; Naulet, N.; Martin, G. J. *J. Agric. Food Chem.* **1997**, *45*, 1844–1848.

(24) Guy, R. G. In *The Chemistry of Cyanates and Their Thio Derivatives*; Patai, S., Ed.; John Wiley & Sons, Inc.: New York, 1977; Part 2, pp 819−886.

(25) (a) Gerlich, G. *Justus Liebigs Ann. Chem.* **1875**, *178*, 80–91. (b) Smith, P. A. S.; Emerson, D. W. *J. Am. Chem. Soc.* **1960**, *82*, 3076–3082. (c) Gurudutt, K. N.; Rao, S.; Srinivas, P. *Indian J. Chem.* **1991**, *30B*, 343–344.

(26) (a) Nedolya, N. A.; Brandsma, L.; Verkruijssse, H. D.; Trofimov, B. A. *Tetrahedron Lett.* **1997**, *38*, 7247–7248. (b) Nedolya, N. A.; Brandsma, L.; Trofimov, B. A. *Russ. J. Org. Chem.* **1998**, *34*, 900–901. (c) Trofimov, B. A. *J. Heterocycl. Chem.* **1999**, *36*, 1469–1490. (d) Klyba, L. V.; Bochkarev, V. N.; Brandsma, L.; Nedolya, N. A.; Trofimov, B. A. *Russ. J. Gen. Chem.* **1999**, *69*, 1805–1809.

(27) Brückner, C.; Posakony, J. J.; Johnson, C. K.; Boyle, R. W.; James, B. R.; Dolphin, D. *J. Porphyrins Phthalocyanines* **1998**, *2*, 455–465.

SCHEME 2

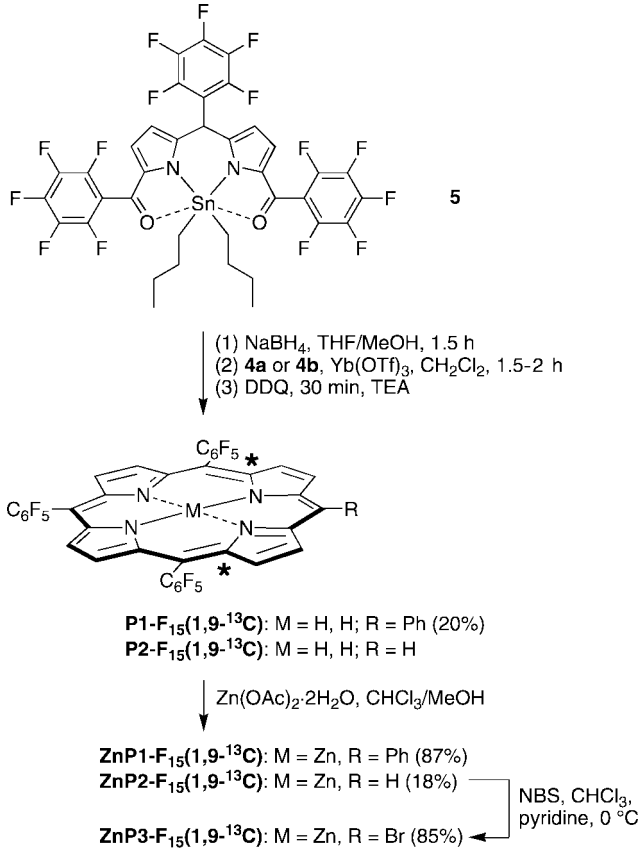

group had been cleaved as shown by ^{1}H NMR and mass spectrometric analyses. The loss of the iodo group precluded use of the Sonogashira route outlined in Chart 4; however, the phenyldipyrromethane (**4a**) so obtained provided the precursor for an additional benchmark porphyrin for dyad studies. On the other hand, hydrodesulfurization of the more robust **3b** gave dipyrromethane **4b** in 29% overall yield (from pyrrole **2**). For both labeled dipyrromethanes (**4a**, **4b**), the ^{1}H resonance from the α-protons was characteristic: in **4a** a doublet of multiplets was observed at 6.66 ppm (^{1}H−^{13}C *J*-coupling of 184.8 Hz), and likewise, for **4b** the signal observed was 6.69 ppm Hz (^{1}H−^{13}C *J*-coupling of 184.4 Hz). The appearance of this resonance as a doublet of multiplets is due to the ^{13}C incorporation at the α-loci. Additionally, *g*HETCOR and *g*HSQC experiments indicated the correlation of the two signals corresponding to the α-protons with the enhanced signal of the ^{13}C atom. The values of the chemical shift and coupling constants for the dipyrromethanes agree with expectations on the basis of comparison with the analogous 2-methylpyrrole.[28]

Porphyrins bearing ^{13}C labels were prepared by condensation of a ^{13}C-labeled dipyrromethane (**4a**, **4b**) and a dipyrromethanedicarbinol (Scheme 2). The dibutyltin complex of the tris(pentafluorophenyl)-substituted 1,9-diacyldipyrromethane (**5**)[29] was reduced with $NaBH_4$ to give the dipyrromethane−dicarbinol, which upon condensation[18,30] with **4a** or **4b** in the presence of

SCHEME 3

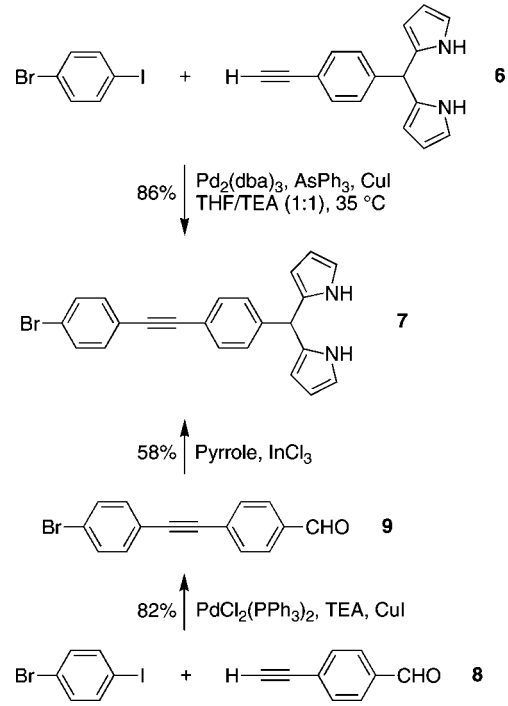

$Yb(OTf)_3$ in CH_2Cl_2 gave the corresponding porphyrin **P1-F$_{15}$(1,9-^{13}C)** (20%) or **P2-F$_{15}$(1,9-^{13}C)** (crude form). Subsequent metalation with zinc acetate gave the corresponding zinc porphyrin **ZnP1-F$_{15}$(1,9-^{13}C)** (87% yield) or **ZnP2-F$_{15}$(1,9-^{13}C)** (18% overall yield). Bromination[31] of porphyrin **ZnP2-F$_{15}$(1,9-^{13}C)** with NBS at 0 °C proceeded regioselectively (as evidenced by the disappearance of the singlet for the meso-H, $\delta = 10.43$ ppm) to give the *meso*-bromoporphyrin **ZnP3-F$_{15}$(1,9-^{13}C)** in 85% yield. Each porphyrin shown in Scheme 2 contains ^{13}C atoms at the 1- and 9-positions of the macrocycle.

3. Unlabeled Porphyrin Monomer. For the Suzuki coupling strategy, the unlabeled porphyrin building block must contain a boronate-derivatized diphenylethyne linker. The corresponding dipyrromethane was prepared as shown in Scheme 3. The known ethynylphenyldipyrromethane **6**[17] was coupled with 1-bromo-4-iodobenzene under Sonogashira conditions [THF/triethylamine (TEA) (1:1) in the presence of $Pd_2(dba)_3$, $AsPh_3$ and CuI] to afford dipyrromethane **7** in 86% yield (Scheme 3). A complementary route to dipyrromethane **7** employed Pd-mediated coupling of 4-ethynylbenzaldehyde (**8**)[32] with 1-bromo-4-iodobenzene and $PdCl_2(PPh_3)_2$, TEA, and CuI in benzene at room temperature to obtain aldehyde **9** in 82% yield. Aldehyde **9** is known[33] but with limited characterization data. Condensation of aldehyde **9** with excess pyrrole in the presence of $InCl_3$[22] afforded dipyrromethane **7** in 58% yield.

The required A_3B-porphyrin building block was prepared as shown in Scheme 4. Thus, reduction of **5** gave the corresponding dipyrromethane−dicarbinol, which upon condensation[18,30] with dipyrromethane **7** gave the free base porphyrin bearing the 1-bromo-*p*-diphenylethyne moiety. Subsequent zinc insertion

(28) Chadwick, D. J. In *Pyrroles. Part One. The Synthesis and the Physical and Chemical Aspects of the Pyrrole Ring*; Jones, R. A., Ed.; John Wiley & Sons, Inc.: New York, 1990; pp 1−103.

(29) Tamaru, S.-I.; Yu, L.; Youngblood, W. J.; Muthukumaran, K.; Taniguchi, M.; Lindsey, J. S. *J. Org. Chem.* **2004**, *69*, 765–777.

(30) Geier, G. R., III; Callinan, J. B.; Rao, P. D.; Lindsey, J. S. *J. Porphyrins Phthalocyanines* **2001**, *5*, 810–823.

(31) Tomizaki, K.-Y.; Lysenko, A. B.; Taniguchi, M.; Lindsey, J. S. *Tetrahedron* **2004**, *60*, 2011–2023.

(32) Austin, W. B.; Bilow, N.; Kelleghan, W. J.; Lau, K. S. Y. *J. Org. Chem.* **1981**, *46*, 2280–2286.

(33) Terazono, Y.; Liddell, P. A.; Garg, V.; Kodis, G.; Brune, A.; Hambourger, M.; Moore, A. L.; Moore, T. A.; Gust, D. *J. Porphyrins Phthalocyanines* **2005**, *9*, 706–723.

SCHEME 4

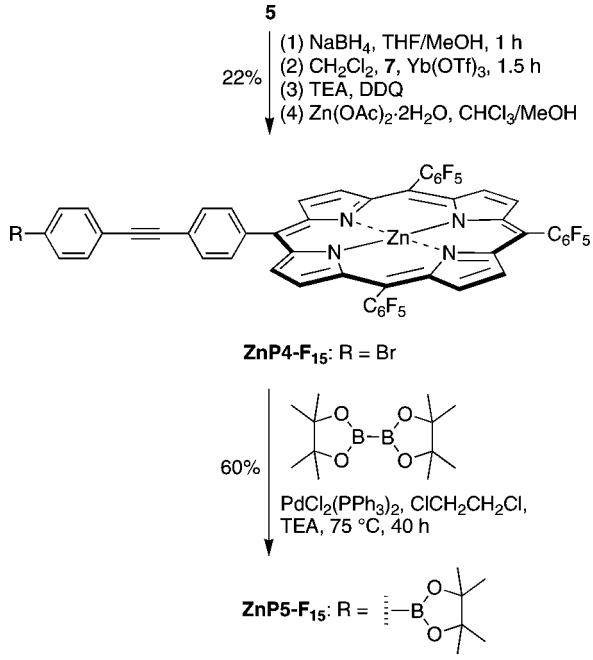

SCHEME 5

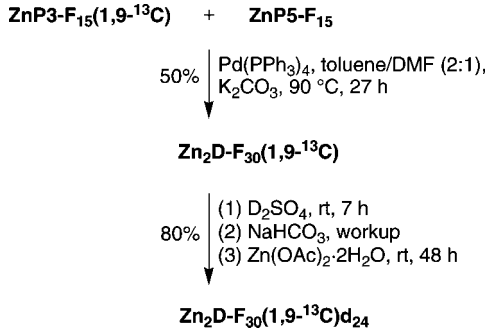

gave porphyrin **ZnP4-F$_{15}$** in 22% yield. Finally, borylation[34] of **ZnP4-F$_{15}$** by treatment with bis(pinacolato)diboron, $PdCl_2(PPh_3)_2$ and TEA at 75 °C for 40 h afforded **ZnP5-F$_{15}$** in 60% yield.

4. Porphyrin Dyads. The isotopically labeled porphyrin **ZnP3-F$_{15}$(1,9-^{13}C)** and unlabeled porphyrin **ZnP5-F$_{15}$** were reacted under Suzuki conditions,[20] which consist of $Pd(PPh_3)_4$ and K_2CO_3 at 90 °C for 27 h (Scheme 5). Analytical-scale size-exclusion chromatography (SEC)[16] was employed to monitor the reaction and to assess the purity of the dyad. Purification by a series of three columns (adsorption chromatography, preparative SEC, and adsorption chromatography) afforded the isotopically labeled porphyrin dyad **Zn$_2$D-F$_{30}$(1,9-^{13}C)** in 50% yield.

A β-deuteriated analogue of dyad **Zn$_2$D-F$_{30}$(1,9-^{13}C)** was sought for EPR studies. The use of perdeuteriated porphyrin monomers in the synthesis of a perdeuteriated triply fused porphyrin dimer has been reported.[35] In our case, however, various Pd-mediated coupling reactions (Suzuki, borylation) with β-deuteriated porphyrin building blocks (e.g., analogues of **ZnP3-F$_{15}$(1,9-^{13}C)** and **ZnP5-F$_{15}$**) resulted in loss of significant amounts of the deuterium labels. The failure of the building-block approach eventually prompted examination of direct deuteriation of the dyad **Zn$_2$D-F$_{30}$(1,9-^{13}C)**. Treatment of **Zn$_2$D-F$_{30}$(1,9-^{13}C)** with TFA-*d*, TFA-*d*/D_2O, or acetic acid-d_4 resulted only in demetalation of the zinc porphyrins, whereas D_2SO_4 at 150 °C gave higher molecular weight side products. To our delight, treatment of **Zn$_2$D-F$_{30}$(1,9-^{13}C)** with D_2SO_4 at room temperature for 7 h afforded the exhaustively deuteriated dyad, wherein the 16 protons at the pyrrole positions and the 8 protons of the diphenylethyne linker underwent exchange. Exchange of porphyrin *meso*-aryl protons under such conditions has been reported.[36] Remetalation with zinc acetate afforded **Zn$_2$D-F$_{30}$(1,9-^{13}C)d$_{24}$** in 80% overall yield and 95% isotopic purity. The extensive level of deuterium incorporation and the absence of unexchanged protons precluded characterization by ^{1}H NMR spectroscopy. Characterization was achieved by absorption spectroscopy, fluorescence spectroscopy, laser-desorption mass spectrometry in the absence of a matrix (LD-MS),[37] and ^{13}C NMR spectroscopy. Substitution of H atoms with D atoms is known to affect the ^{13}C NMR spectra.[38] The ^{13}C signal of **Zn$_2$D-F$_{30}$(1,9-^{13}C)d$_{24}$** appears as a multiplet at 150.1−150.2 ppm. This route to per deuteriated dyads may be useful because the resulting array contains only two nuclei with spin 1/2, which is anticipated to simplify the EPR spectra, although the amounts of material obtained in the present case were quite limited.

5. Porphyrin Benchmarks. EPR studies required the synthesis of porphyrin monomers for assessing the magnitude of the contribution of ^{1}H hyperfine interactions and for comparison with the properties of the two dyads. One benchmark was perdeuterio-*meso*-tetrakis(pentafluorophenyl)porphyrin, which could be prepared by condensation of pentafluorobenzaldehyde and either pyrrole-d_5[39] or pyrrole itself (with in situ deuteriation).[36] The time-honored method for meso-deuteriation of octaethylporphyrin entails treatment with D_2SO_4 at room temperature.[40] Treatment of *meso*-tetrakis(pentafluorophenyl)porphyrin (**P6-F$_{20}$**) with D_2SO_4 at 150 °C for 22 h resulted in deuterium exchange of the pyrrole hydrogens; aqueous workup afforded the desired **P6-F$_{20}$d$_8$** (Scheme 6). A strong signal at −2.93 ppm and a weak signal at 8.92 ppm were observed in the ^{1}H NMR spectrum, and the LD-MS spectrum exhibited a peak at m/z = 982.4. Integration of the NMR peaks indicated the porphyrin **P6-F$_{20}$d$_8$** was 97% isotopically pure. Subsequent zinc metalation gave **ZnP6-F$_{20}$d$_8$** quantitatively.

A second benchmark was a β-deuteriated A_3B-porphyrin monomer bearing ^{13}C atoms at the 1,9-positions. Treatment of **ZnP1-F$_{15}$(1,9-^{13}C)** to mild deuteriation conditions such as acetic acid-d_4 or TFA-*d* at room temperature for 1 week, TFA-*d* at 60 °C for 48 h, or D_2SO_4 at room temperature proved to be unsuccessful for the β-deuteriation. Treatment with D_2SO_4 at 110 °C for 48 h followed by remetalation with zinc acetate

(34) (a) Yu, L.; Muthukumaran, K.; Sazanovich, I. V.; Kirmaier, C.; Hindin, E.; Diers, J. R.; Boyle, P. D.; Bocian, D. F.; Holten, D.; Lindsey, J. S. *Inorg. Chem.* **2003**, *42*, 6629–6647. (b) Ishiyama, T.; Murata, M.; Miyaura, N. *J. Org. Chem.* **1995**, *60*, 7508–7510. (c) Chng, L. L.; Chang, C. J.; Nocera, D. G. *J. Org. Chem.* **2003**, *68*, 4075–4078.

(35) Frampton, M. J.; Accorsi, G.; Armaroli, N.; Rogers, J. E.; Fleitz, P. A.; McEwan, K. J.; Anderson, H. L. *Org. Biomol. Chem.* **2007**, *5*, 1056–1061.

(36) Gross, Z.; Kaustov, L. *Tetrahedron Lett.* **1995**, *36*, 3735–3736.

(37) (a) Fenyo, D.; Chait, B. T.; Johnson, T. E.; Lindsey, J. S. *J. Porphyrins Phthalocyanines* **1997**, *1*, 93–99. (b) Srinivasan, N.; Haney, C. A.; Lindsey, J. S.; Zhang, W.; Chait, B. T. *J. Porphyrins Phthalocyanines* **1999**, *3*, 283–291.

(38) (a) Hansen, P. E. *Prog. NMR Spectrosc.* **1981**, *14*, 175–296. (b) Söderman, O. *J. Magn. Reson.* **1986**, *68*, 296–302.

(39) (a) Shirazi, A.; Goff, H. M. *J. Am. Chem. Soc.* **1982**, *104*, 6318–6322. (b) Asano, M. S.; Abe, H.; Kaizu, Y. *J. Label. Compd. Radiopharm.* **2006**, *49*, 595–601.

(40) Fuhrhop, J.-H.; Smith, K. M. In *Porphyrins and Metalloporphyrins*; Smith, K. M., Ed.; Elsevier: Amsterdam, 1975; pp 757−869.

(41) (a) Spellane, P. J.; Gouterman, M.; Antipas, A.; Kim, S.; Liu, Y. C. *Inorg. Chem.* **1980**, *19*, 386–391. (b) Collman, J. P.; Hampton, P. D.; Brauman, J. I. *J. Am. Chem. Soc.* **1990**, *112*, 2986–2998.

SCHEME 6

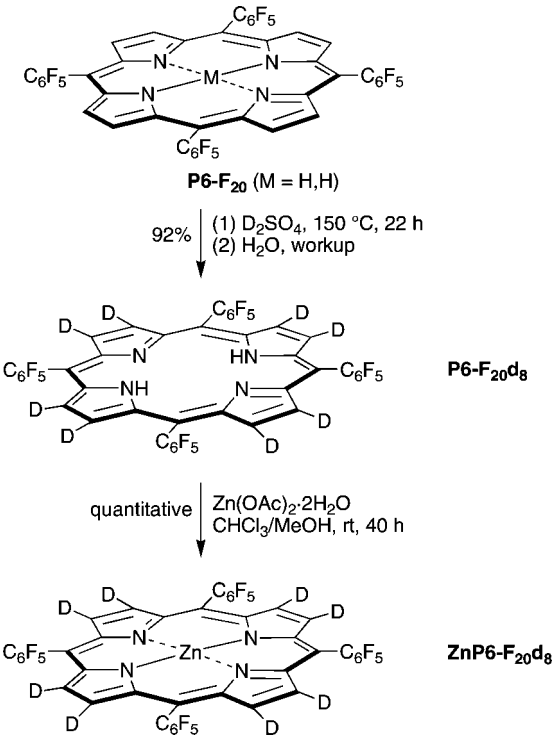

SCHEME 7

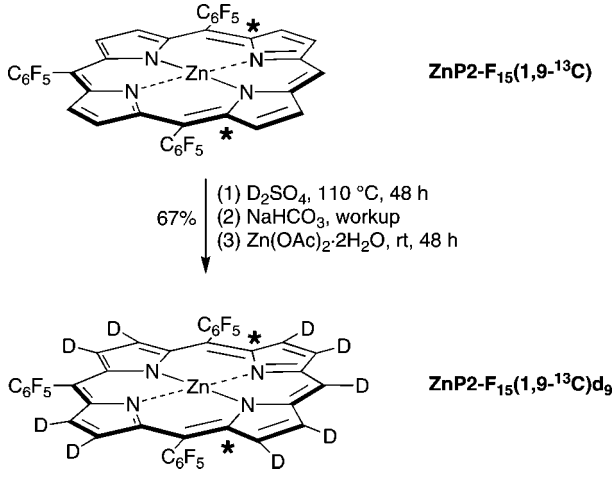

afforded the corresponding β-deuteriated porphyrin **ZnP2-F$_{15}$(1,9-^{13}C)d$_9$** in 67% yield (Scheme 7). Analysis by negative ion FAB-MS gave an observable signal but the intensity was insufficient for high-resolution data, whereas MALDI-MS in the negative ion mode gave a good quality signal albeit at low resolution. The ^{13}C resonances for all isotopically labeled compounds prepared herein are presented in Table 1.

All of the porphyrin monomers suitable herein as benchmarks for EPR spectroscopy are shown in Chart 5. **ZnP1-F$_{15}$(1,9-^{13}C)** and **ZnP2-F$_{15}$(1,9-^{13}C)** were prepared as shown in Scheme 2. **ZnP2-F$_{15}$(1,9-^{13}C)d$_9$** was prepared from **ZnP2-F$_{15}$(1,9-^{13}C)** as shown in Scheme 7. **ZnP6-F$_{20}$** was obtained by metalation of the free base porphyrin **P6-F$_{20}$**.[41] **ZnP6-F$_{20}$d$_8$** was prepared as shown in Scheme 6. **ZnP7-F$_{15}$** was prepared as described in the literature.[10]

II. EPR Studies. Monocations of the porphyrin monomers and dyads were prepared by standard electrochemical techniques.[42] Room-temperature EPR spectra of the monomer [**ZnP7-F$_{15}$**]$^+$ and the dyad [**Zn$_2$D-F$_{30}$**]$^+$ are shown in Figure 2. As we have previously reported, the spectra of neither [**ZnP7-F$_{15}$**]$^+$ nor [**Zn$_2$D-F$_{30}$**]$^+$ exhibit any resolved hyperfine structure, and the peak-to-peak line widths (ΔH_{pp}) for the two monocations are quite similar.[10] The finding that the peak-to-peak line widths (and underlying hyperfine splittings) are similar for [**Zn$_2$D-F$_{30}$**]$^+$ and [**ZnP7-F$_{15}$**]$^+$ suggests that ground-state hole transfer in [**Zn$_2$D-F$_{30}$**]$^+$ is slow on the EPR time scale. If hole transfer in [**Zn$_2$D-F$_{30}$**]$^+$ were rapid on the EPR time scale, the line width

TABLE 1. ^{13}C Resonances of Labeled Compounds

entry	compd type	compd	^{13}C resonance (δ, ppm)
1	isothiocyanate	**1**	132.4
2	pyrrole	**2**	121.5
3	dipyrromethane	**3a**	121.6
4	dipyrromethane	**3b**	121.0
5	dipyrromethane	**4a**	117.4
6	dipyrromethane	**4b**	117.4
7	porphyrin	**ZnP1-F$_{15}$(1,9-^{13}C)**	150.1
8	porphyrin	**ZnP2-F$_{15}$(1,9-^{13}C)**	150.2
9	porphyrin	**ZnP3-F$_{15}$(1,9-^{13}C)**	150.5
10	dyad	**Zn$_2$D-F$_{30}$(1,9-^{13}C)**	150.2
11	dyad	**Zn$_2$D-F$_{30}$(1,9-^{13}C)d$_{24}$**	150.16−150.22
12	porphyrin	**ZnP2-F$_{15}$(1,9-^{13}C)d$_9$**	150.11−150.18

CHART 5

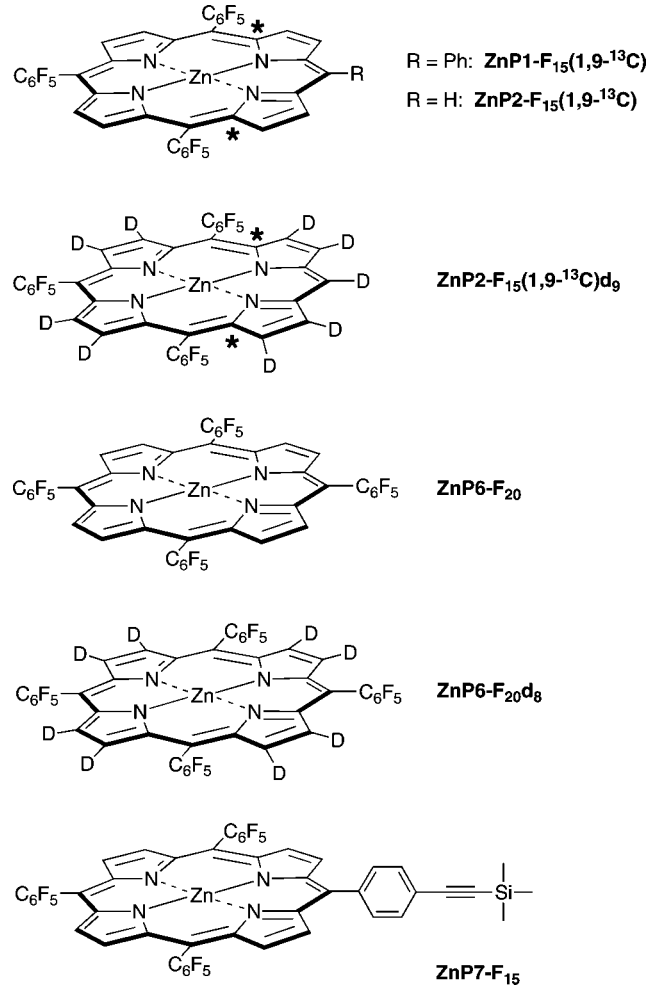

(42) Yang, S. I.; Seth, J.; Strachan, J.-P.; Gentemann, S.; Kim, D.; Holten, D.; Lindsey, J. S.; Bocian, D. F. *J. Porphyrins Phthalocyanines* **1999**, *3*, 117–147.

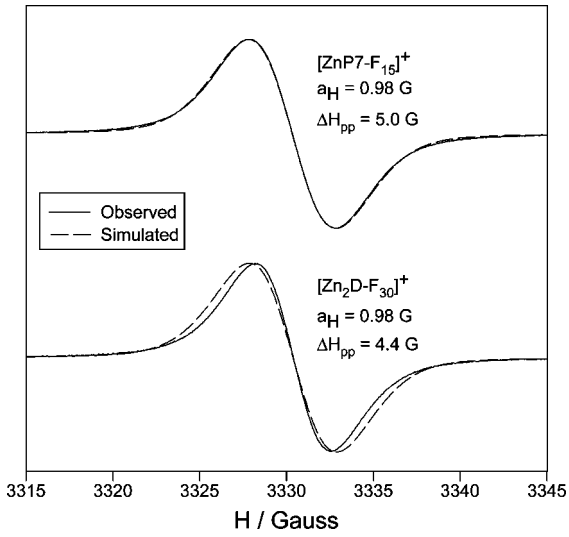

FIGURE 2. Room-temperature EPR spectra of $[\mathbf{ZnP7\text{-}F_{15}}]^+$ and $[\mathbf{Zn_2D\text{-}F_{30}}]^+$.

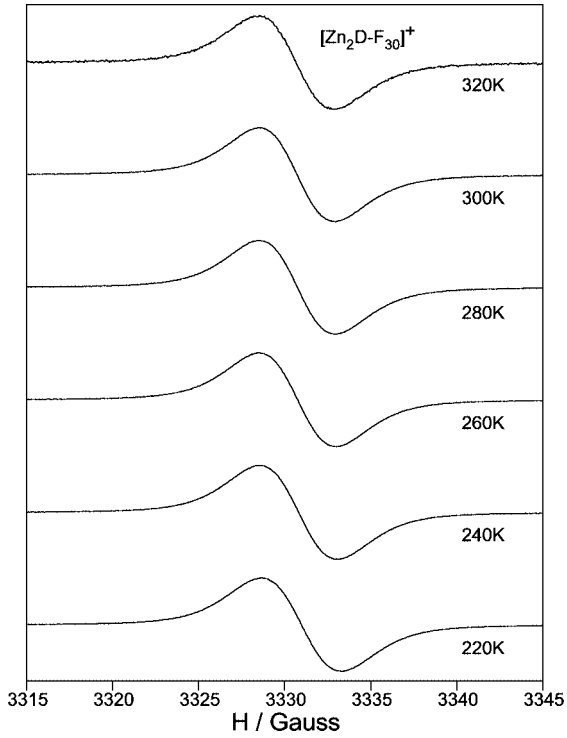

FIGURE 3. Temperature dependence of the EPR spectra of $[\mathbf{Zn_2D\text{-}F_{30}}]^+$.

for the dyadic monocation would be expected to be narrower than that of the monomeric monocation.[10] Elevating the temperature to 320 K (or lowering the temperature to 220 K) has no effect on the peak-to-peak line width of $\mathbf{[Zn_2D\text{-}F_{30}]^+}$, as is illustrated in Figure 3, which shows the EPR spectra of the dyadic monocation over the range 220 to 320 K. [Note that temperatures higher than 320 K cannot be accessed owing to boiling of the solvent (CH_2Cl_2).] Thus, hole transfer in $\mathbf{[Zn_2D\text{-}F_{30}]^+}$ appears to be slow under all of the conditions used to acquire the EPR spectra. However, as noted in the Introduction, deriving a definitive lower limit on the rate is difficult in this case because (1) the hyperfine coupling to the ^{14}N nuclei of the pyrrole rings is negligible for the $^2A_{1u}$ monocation and (2) the magnitude of the coupling to the ^1H nuclei at the β-pyrrole

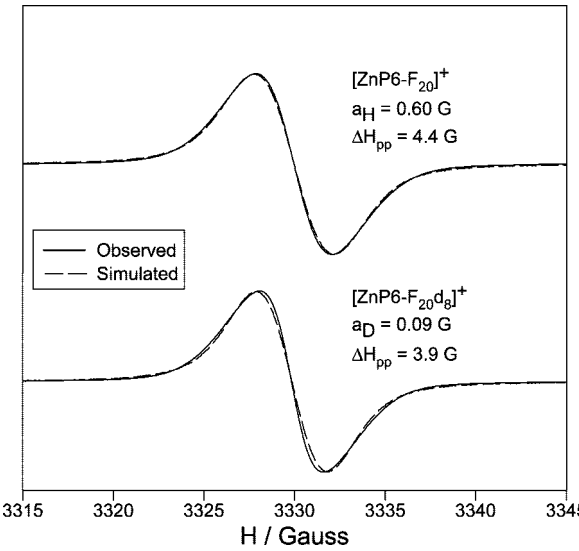

FIGURE 4. Room-temperature EPR spectra of $[\mathbf{ZnP6\text{-}F_{20}}]^+$ and $[\mathbf{ZnP6\text{-}F_{20}d_8}]^+$.

positions is somewhat uncertain. Therefore, the additional studies described below were performed.

The issues regarding the magnitude of the ^1H hyperfine coupling are resolved by studies of the various deuteriated porphyrins. This point is illustrated in Figure 4, which compares the EPR spectra of one pair of representative monomers, $[\mathbf{ZnP6\text{-}F_{20}}]^+$ and $[\mathbf{ZnP6\text{-}F_{20}d_8}]^+$. These spectral data show that deuteriation of the β-pyrrole positions results in very little change in the overall EPR line width. Similar results were obtained for all of the other deuteriated versus protonated complexes (data not shown). Self-consistent spectral simulations for $[\mathbf{ZnP6\text{-}F_{20}}]^+$ and $[\mathbf{ZnP6\text{-}F_{20}d_8}]^+$ ($a_D/a_H = 0.15$ and a fixed line width[12]) indicate that the largest value possible for the ^1H hyperfine is significantly smaller than the inhomogeneous line width. Thus, the β-pyrrole ^1H hyperfine coupling cannot be used reliably as a hyperfine clock to assess the hole-transfer characteristics of $[\mathbf{Zn_2D\text{-}F_{30}}]^+$.

The assessment of the ground-state hole-transfer characteristics of $[\mathbf{Zn_2D\text{-}F_{30}}]^+$ is resolved by incorporation of the ^{13}C labels at the two equivalent α-pyrrole positions. This is illustrated in Figure 5, which compares the room-temperature EPR spectra of the monomer $[\mathbf{ZnP2\text{-}F_{15}(1,9\text{-}^{13}C)d_9}]^+$ and dyad $[\mathbf{Zn_2D\text{-}F_{30}(1,9\text{-}^{13}C)}]^+$. The comparison of the spectra of the deuteriated monomer versus protonated dyad is arbitrary; deuteriation has no significant effect on the line shape of any of the monomers or dyads. [Note that the lower S/N observed for the isotopically labeled complexes (Figure 5) versus the unlabeled complexes (Figure 2) is due to the smaller quantities available for the former complexes.] Inspection of Figure 5 reveals that the line shape of the monomeric cation, while exhibiting no resolved hyperfine structure, is broader than that of $[\mathbf{ZnP7\text{-}F_{15}}]^+$ (and the other benchmark monomers), which lack the α-^{13}C labels (Figure 2). Self-consistent spectral simulations for $[\mathbf{ZnP7\text{-}F_{15}}]^+$ and $[\mathbf{ZnP2\text{-}F_{15}(1,9\text{-}^{13}C)d_9}]^+$ indicate that the $a_{^{13}C}$ is ~2.35 G (~6.2 MHz). The value of $a_{^{13}C}$ ~6.2 MHz observed for α-^{13}C-labeled $[\mathbf{ZnP2\text{-}F_{15}(1,9\text{-}^{13}C)d_9}]^+$ is smaller than the value of $a_{^{13}C}$ ~16 MHz observed for the monocations of the meso-^{13}C-labeled porphyrins shown in Chart 2,[13] as expected because the spin density at the α-pyrrole C atoms of the $^2A_{1u}$ cations is significantly less than that at the meso-C atoms of the $^2A_{2u}$ cations.[12]

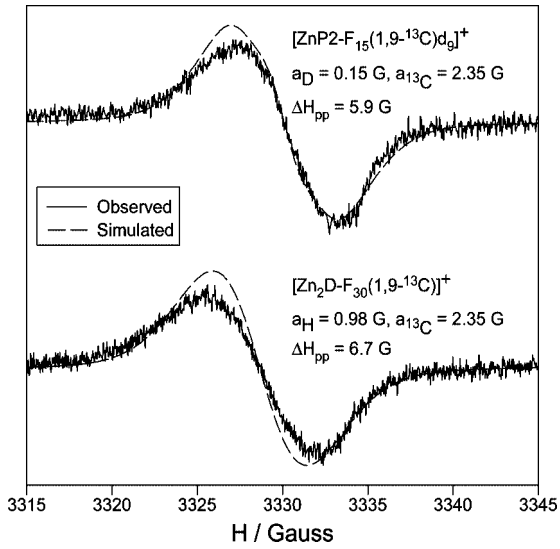

FIGURE 5. Room-temperature EPR spectra of **[ZnP2-F$_{15}$(1,9-^{13}C)d$_9$]$^+$** and **[Zn$_2$D-F$_{30}$(1,9-^{13}C)]$^+$**.

Further inspection of Figure 5 reveals that the line shape of **[Zn$_2$D-F$_{30}$(1,9-^{13}C)]$^+$** is generally similar to that of **[ZnP2-F$_{15}$(1,9-^{13}C)d$_9$]$^+$**. Simulations of the spectrum of the dyad indicate that the line shape can be accounted for by a superposition of the EPR spectra of two monomeric monocations — one of normal isotopic composition, the other containing two α-^{13}C labels with $a_{^{13}C}$ ~2.35 G. In other words, the EPR spectrum of the dyadic monocation is the same as that of a 50/50 mixture of two monomers each exhibiting hyperfine couplings characteristic of one or the other half of the isotopically unsymmetrical dyad. These characteristics of the EPR spectrum, particularly the fact that the ^{13}C hyperfine coupling in the dyadic monocation is the same as that of a monomeric monocation, definitively show that hole transfer is slow ($<10^6$ s^{-1}) on the EPR time scale for the $^2A_{1u}$ dyadic monocation. If the hole transfer were rapid on the EPR time scale, the line shape would instead be characteristic of a single species (rather than two species) wherein the effective hyperfine couplings of all nuclei are one-half the value observed for a monomer.[10] The slower hole-transfer rate for the $^2A_{1u}$ monocation **[Zn$_2$D-F$_{30}$]$^+$** compared with those of the $^2A_{2u}$ monocations **[Zn$_2$D-Mes]$^+$** and **[Zn$_2$D-SWT]$^+$** is attributed to the fact that in the former dyad, the linker site (meso position) is at a position of negligible electron/spin density (nodal plane) in the HOMO, whereas in the latter dyads, the linker is at a position of large electron/spin density in the HOMO (Figure 1).

Conclusions

A strategy has been demonstrated for assessing the ground-state hole-transfer rate in cationic π-radical systems wherein the redox-active constituents lack substantial nuclear-hyperfine couplings. The strategy entails introduction of ^{13}C labels at sites of substantial electron/spin density in the HOMO. For electron-deficient porphyrins, the HOMO is a_{1u}, wherein the largest electron/spin density resides at the α-pyrrolic carbons; negligible electron/spin density resides at the meso-carbons or pyrrole nitrogens, both of which are in nodal planes of the HOMO. A new synthetic approach, beginning with ^{13}C-labeled KSCN, was devised to prepare a dipyrromethane bearing ^{13}C labels specifically at the two α- (1- and 9-) positions. The dipyrromethane-*1,9-^{13}C* could then be employed in standard methods for porphyrin formation followed by elaboration of the regiospecifically labeled porphyrin into dyads. Examination of the resulting meso-diphenylethyne-linked porphyrin dyads by EPR spectroscopy established that the hole-transfer rate is $<10^6$ s^{-1} at room temperature. This hole-transfer rate is at least 50-fold slower than that for meso-diphenylethyne-linked, electron-rich porphyrin dyads, wherein the HOMO is a_{2u}, which has substantial electron/spin density at the meso-carbons. The new synthetic methodology for preparing 1,9-^{13}C-labeled porphyrins provides an entrée for examining hole transfer in other types of electron-deficient porphyrin arrays in which different aspects of the molecular structure, such as the site of linker attachment, are varied.

Experimental Section

Electrochemistry. The electrochemical measurements (cyclic voltammetry and bulk electrolysis) were performed using techniques and instrumentation previously described.[42] The solvent was CH_2Cl_2 containing 0.1 M Bu_4NPF_6 as the supporting electrolyte. The bulk oxidized complexes were prepared in a glovebox using techniques previously described. Upon oxidation, the samples were transferred to an EPR tube and sealed in the glovebox.

EPR Spectroscopy. The EPR spectra were recorded on an X-band spectrometer (Bruker EMX) equipped with an NMR gaussmeter and microwave frequency counter. The EPR spectra were obtained on samples that were typically 0.2 mM at both ambient and cryogenic temperatures. The microwave power and magnetic field modulation amplitude were typically 5.7 mW and 0.32 G, respectively.

Allyl Isothio(cyanate-^{13}*C*) (1). A sample of KS^{13}CN (99% isotopic purity) was dried overnight in a high vacuum oven at 140 °C. A solution of allyl bromide (0.760 mL, 9.00 mmol) in dry THF (9 mL, 1 M) was treated with KS^{13}CN (1 g, 0.01 mol) and heated to 55 °C. The reaction was monitored by TLC, GC−MS, ^{1}H NMR, and ^{13}C NMR analyses. After 3 days, the reaction mixture was cooled to room temperature and filtered. The filtrate was concentrated under reduced pressure at room temperature (to avoid loss of product; expected bp = 150 °C) to a yellow oil (0.776 g, 86% yield, 99% purity according to GC−MS and ^{1}H NMR spectroscopy): ^{1}H NMR δ 4.13−4.17 (m, 2H), 5.27−5.30 (m, 1H), 5.38−5.42 (m, 1H), 5.81−5.88 (m, 1H); ^{13}C NMR δ 47.1, 117.7, 130.5, 132.4 (enh); GC−MS t_R = 4.74 min, *m/z* = 100; calcd 100.0 ($C_3{}^{13}CH_5NS$).

CAUTION. *Allyl isothiocyanate is reported to be toxic and flammable,*[23] is a strong lachrymator, and should be handled in a well-vented hood with care.

2-(Methylthio)pyrrole-*2*-^{13}*C* (2). Following a reported procedure[26] with modification, diisopropylamine (855 μL, 6.00 mmol) was added at room temperature under argon to a mixture of *t*-BuOK (673 mg, 6.00 mmol) in dry THF (3.75 mL, 0.800 M), and the mixture was cooled to −100 °C (using a cooling bath of ethanol and liquid nitrogen). A sample of *n*-BuLi (3.75 mL, 6.0 mmol, 1.6 M in hexanes) was added dropwise, whereupon the mixture turned yellow. The reaction vessel was placed in a cooling bath consisting of dry ice and acetonitrile. When the reaction mixture attained −40 °C, a solution of allyl isothiocyanate **1** (300 mg, 3.00 mmol, in 2.40 mL of dry THF, 1.25 M) was added dropwise via a 25 μL syringe over a period of 50 min, maintaining the temperature at −35 to −25 °C. The cooling bath was removed, and after reaching room temperature, the reaction mixture was heated to 40 °C for 40 min. The heat source was removed and H_2O (480 μL) was added. Stirring was continued at room temperature for 35 min. Then CH_3I (155 μL, 2.70 mmol) was added to the reaction vessel. The reaction mixture was heated at 45 °C for 40 min. The reaction mixture was allowed to cool to room temperature, treated with cold H_2O (5 mL), and extracted with diethyl ether. The organic phase was dried (K_2CO_3) and concentrated to a brown oil. Column chromatography

[silica hexanes/CH_2Cl_2 (1:2)] gave a yellow oil (172 mg, 56%): ^{1}H NMR δ 2.33 (d, J = 4.8 Hz, 3H), 6.19−6.22 (m, 1H), 6.34−6.37 (m, 1H), 6.78−6.81 (m, 1H), 8.23 (br, 1H); ^{13}C NMR δ 21.9, 114.8, 115.5, 120.18, 121.5 (enh); FAB-MS obsd 115.0442, calcd 115.0405 [(M + H)$^+$; M = $C_4{}^{13}CH_7NS$]; GC−MS t_R = 9.18 min; m/z = 114. Note: Dimerization of allyl isothiocyanate is a significant possible side reaction. Departure from the specified conditions (temperature, addition, concentrations, stoichiometry, etc.) can lead to lower yields.

1,9-Bis(methylthio)-5-(4-iodophenyl)dipyrromethane-*1,9*-^{13}*C* (3a). Following a reported procedure,[19] a mixture of pyrrole **2** (285 mg, 2.50 mmol) and 4-iodobenzaldehyde (290 mg, 1.25 mmol) was treated with $InCl_3$ (58 mg, 0.25 mmol) and stirred at room temperature under an argon atmosphere. After 52 h, TLC analysis showed the complete consumption of the starting material. The reaction mixture was treated with hexanes/THF (6 mL, 2:1) and filtered. The filtrate was concentrated to dryness. Column chromatography [silica, hexanes/CH_2Cl_2 (1:2)] afforded a yellow-orange solid (165 mg, 30%): mp 109−112 °C; GC t_R = 24.9 min; ^{1}H NMR δ 2.29 (d, J = 4.8 Hz, 6H), 5.31 (s, 1H), 5.81−5.85 (m, 2H), 6.24−6.27 (m, 2H), 6.93 (d, J = 8.3 Hz, 2H), 7.64 (d, J = 8.3 Hz, 2H), 7.90 (br s, 2H); ^{13}C NMR δ 21.9, 44.1, 92.9, 109.5, 115.2, 115.9, 120.6, 121.6 (enh), 130.6, 133.8, 138.1, 141.0; FAB-MS obsd 441.9933, calcd 441.9945 ($C_{15}{}^{13}C_2H_{17}IN_2S_2$).

5-Phenyldipyrromethane-*1,9*-^{13}*C* (4a). Following a reported procedure,[19] Raney nickel (∼1.5 g, slurry in EtOH) was added to a solution of **3a** (150 mg, 0.339 mmol) in EtOH (15 mL) at room temperature. After 30 min, TLC indicated the complete consumption of **3a** and the presence of the product. The reaction mixture was treated with hexanes/THF (2:1) and filtered through a Celite pad. The filter cake was washed with diethyl ether. The filtrate was concentrated. Column chromatography (silica, CH_2Cl_2) gave a gray solid (30 mg, 40%): mp 99−102 °C; ^{1}H NMR δ 5.51 (s, 1H), 5.90−5.93 (m, 2H), 6.13−6.18 (m, 2H), 6.69 (dm, J = 184.4 Hz, 2H), 7.18−7.24 (m, 2H), 7.28−7.35(m, 3H), 7.93 (br s, 2H); ^{13}C NMR δ 44.1, 107.4, 108.3, 108.9, 116.7, 117.4 (enh), 118.2, 127.2, 128.6, 128.9; ESI-MS obsd 225.1297, calcd 225.1296 [(M + H)$^+$; M = $C_{13}{}^{13}C_2H_{14}N_2$].

Dipyrromethane-*1,9*-^{13}*C* (4b). Following a reported procedure,[19] a sample of pyrrole **2** (0.179 g, 1.57 mmol) and paraformaldehyde (22 mg, 0.75 mmol) was heated at 50 °C until a homogeneous mixture was obtained. The mixture was treated with $InCl_3$ (33 mg, 0.15 mmol) and stirred at room temperature for 18 h. The reaction mixture was treated with hexanes/THF (2:1) and filtered. The filter cake was washed with diethyl ether. The filtrate was concentrated to give a crude product with satisfactory characterization data [^{1}H NMR δ 2.31 (d, J = 4.8 Hz, 6H), 3.91 (s, 2H), 5.98−6.01 (m, 2H), 6.25−6.29 (m, 2H), 7.95 (br, 2H); ^{13}C NMR δ 106.6, 108.3, 108.9, 121.0 (enh), 127.6]. The resulting crude mixture was dissolved in THF (4 mL) and treated with Raney nickel (∼200 mg) slurry in THF at room temperature for 45 min. Raney nickel was removed by filtration through a Celite pad. The filter cake was washed with THF. The filtrate was concentrated to dryness. Column chromatography [silica, hexanes/CH_2Cl_2 (1:2)] gave a gray solid (32 mg, 29%): mp 67−70 °C; ^{1}H NMR δ 3.98 (s, 2H), 6.02−6.05 (m, 2H), 6.12−6.17 (m, 2H), 6.66 (dm, J = 184.8 Hz, 2H), 7.83 (br s, 2H); ^{13}C NMR δ 26.6, 106.6, 108.2, 108.9, 116.7, 117.4 (enh), 118.2; GC−MS t_R = 14.17 min, m/z = 148; ESI-MS obsd 149.0985, calcd 149.0983 [(M + H)$^+$, M = $C_7{}^{13}C_2H_{10}N_2$].

5-[4-[2-(4-Bromophenyl)ethynyl]phenyl]dipyrromethane (7). Dipyrromethane **6** (123 mg, 0.500 mmol), 1-bromo-4-iodobenzene (141 mg, 0.500 mmol), $Pd_2(dba)_3$ (14 mg, 0.015 mmol), $AsPh_3$ (36 mg, 0.12 mmol), and CuI (28 mg, 0.15 mmol) were weighed into a 10 mL Schlenk flask which was then pump-purged three times with argon. Dry, degassed THF/TEA (5 mL, 1:1) was added to the Schlenk flask, and the reaction mixture was stirred at 35 °C under argon for 24 h. The solvent was evaporated. Purification by column chromatography (silica, CH_2Cl_2) afforded a gold-yellow solid (172 mg, 86%): mp 132−134 °C; ^{1}H NMR δ 5.48 (s, 1H), 5.90−5.91 (m, 2H), 6.15−6.18 (m, 2H), 6.70−6.72 (m, 2H), 7.19 (d, J = 8.3 Hz, 2H), 7.36−7.39 (m, 2H), 7.45−7.48 (m, 4H), 7.93 (br s, 2H); ^{13}C NMR δ 44.1, 88.6, 90.5, 107.6, 108.8, 117.7, 121.8, 122.4, 122.7, 128.7, 131.8, 132.1, 133.2, 142.8; FAB-MS obsd 400.0564, calcd 400.0575 ($C_{23}H_{17}BrN_2$).

Route 2 to Dipyrromethane 7. Following a reported procedure,[22] a sample of aldehyde **9** (200 mg, 0.701 mmol) and pyrrole (4.8 mL, 70 mmol) was degassed for 10 min. $InCl_3$ (15 mg, 0.070 mmol) was added, and the mixture was stirred at room temperature under argon. After 1.5 h, the reaction mixture was treated with NaOH (84 mg, 2.1 mmol), and the stirring was continued for 1 h. The reaction mixture was filtered, and the filtrate was concentrated. The resulting solid was triturated with hexanes and the volatile components were evaporated. Crystallization from ethanol−water afforded the product as a yellow solid (162 mg, 58%). Characterization data were identical with those described above.

4-[2-(4-Bromophenyl)ethynyl]benzaldehyde (9). Following a reported procedure,[33] a sample of aldehyde **8** (140 mg, 1.06 mmol), 1-bromo-4-iodobenzene (300 mg, 1.06 mmol), $PdCl_2(PPh_3)_2$ (40 mg, 0.025 mmol), and CuI (24 mg, 0.12 mmol) were weighed into a 50 mL Schlenk flask which was then pump-purged three times with argon. Dry, degassed benzene/TEA (7 mL, 3:1) was added to the Schlenk flask, and the reaction mixture was stirred at room temperature under argon for 18 h. The reaction mixture was treated with CH_2Cl_2 followed by 0.1 M HCl. The organic layer was washed (water, brine), separated, and dried (Na_2SO_4). The solvent was evaporated. Purification by column chromatography (silica, CH_2Cl_2) afforded a pale-yellow solid (247 mg, 82%): mp 167−169 °C; ^{1}H NMR δ 7.40−7.44 (m, 2H), 7.50−7.53 (m, 2H), 7.66 (d, J = 8.4 Hz 2H), 7.87 (d, J = 8.1 Hz, 2H), 10.03 (s, 1H); ^{13}C NMR δ 89.8, 92.5, 121.6, 123.6, 129.4, 129.8, 132.0, 132.3, 133.4, 135.8, 191.6; GS−MS t_R = 22.9 min, m/z = 284; ESI-MS obsd 284.9914, calcd 284.9909 [(M + H)$^+$, M = $C_{15}H_9BrO$].

5-Phenyl-10,15,20-tris(pentafluorophenyl)porphyrin-*1,9*-^{13}*C* (P1-F$_{15}$(1,9-^{13}C)). Following general procedures,[18,29,30] reduction of tin complex **5** (100 mg, 0.109 mmol) in THF/MeOH (4.4 mL, 3:1) with $NaBH_4$ (0.161 g, 4.36 mmol) for 1.5 h afforded a yellow solid. The latter was treated with **4a** (24.0 mg, 0.108 mmol) in CH_2Cl_2 (44 mL, 2.5 mM) containing $Yb(OTf)_3$ (90.0 mg, 0.145 mmol) at room temperature for 2 h, followed by oxidation with DDQ (74 mg, 0.32 mmol). The reaction mixture was stirred for 30 min, and TEA (100 μL) was added. Column chromatography (silica, CH_2Cl_2) afforded a purple solid (20 mg, 20%): ^{1}H NMR δ −2.79 (s, 2H), 7.77−7.84 (m, 3H), 8.20−8.22 (m, 2H), 8.79−8.86 (m, 2H), 8.88−8.89 (m, 4H), 8.96−8.99 (m, 2H); ^{13}C NMR δ 150.1 (enh); LD-MS obsd 886.6; FAB-MS obsd 886.1147, calcd 886.1124 ($C_{42}{}^{13}C_2H_{15}F_{15}N_4$); λ_{abs} 418, 511, 541, 587, 642 nm; λ_{em} (λ_{ex} = 418 nm) 650, 720 nm.

5-Phenyl-10,15,20-tris(pentafluorophenyl)porphinatozinc(II)-*1,9*-^{13}*C* (ZnP1-F$_{15}$(1,9-^{13}C)). Following a general procedure,[29] a sample of **P1-F$_{15}$(1,9-^{13}C)** (15 mg, 0.017 mmol) in $CHCl_3$ (3.4 mL) was treated overnight with methanolic $Zn(OAc)_2\cdot 2H_2O$ (18 mg, 0.085 mmol) at room temperature. Column chromatography (silica, CH_2Cl_2) afforded a purple solid (14 mg, 87%): ^{1}H NMR δ 7.78−7.84 (m, 3H), 8.21−8.24 (m, 2H), 8.90−8.93 (m, 2H), 8.97−9.10 (m, 4H), 9.05−9.10 (m, 2H); ^{13}C NMR δ 126.9, 128.3, 130.5, 131.0, 131.8, 132.07, 132.11, 134.61, 134.68, 150.1 (enh), 151.1; LD-MS obsd 948.8; FAB-MS obsd 948.0208, calcd 948.0259 ($C_{42}{}^{13}C_2H_{13}F_{15}N_4Zn$); λ_{abs} 421, 553 nm; λ_{em} (λ_{ex} = 421 nm) 580, 650 nm.

5,10,15-Tris(pentafluorophenyl)porphinatozinc(II)-*1,9*-^{13}*C*(ZnP2-F$_{15}$(1,9-^{13}C)). As described above for **P1-F$_{15}$(1,9-^{13}C)**, reduction of tin complex **5** (186 mg, 0.200 mmol) in dry THF/MeOH (8 mL, 3:1) with $NaBH_4$ (295 mg, 8.00 mmol) for 1.5 h gave a yellow material after workup. The yellow material was dissolved in dry CH_2Cl_2 (80 mL, 2.5 mM) and treated with **4b** (30 mg, 0.20 mmol) and $Yb(OTf)_3$ (164 mg, 0.264 mmol) at room temperature. After 1.5 h, DDQ (136 mg, 0.600 mmol) was added. After 30 min, TEA (180 μL) was added to the reaction mixture. The crude reaction

mixture was passed through a silica pad. The resulting purple solid was dissolved in $CHCl_3$ (5 mL) and treated overnight with methanolic $Zn(OAc)_2 \cdot 2H_2O$ (44 mg, 0.20 mmol, 2.0 mL of MeOH) at room temperature. Column chromatography [silica, hexanes/CH_2Cl_2 (1:1)] afforded a purple solid (32 mg, 18%): ^{1}H NMR δ 9.01−9.07 (m, 6H), 9.52−9.56 (m, 2H) 10.43 (s, 1H); ^{13}C NMR δ 131.3, 131.8, 132.0, 134.4, 150.2 (enh); ESI-MS obsd 873.0013, calcd 873.0019 [$(M + H)^+$, $M = C_{36}{}^{13}C_2H_9F_{15}N_4Zn$]; LD-MS obsd 872.2, 854.2 $(M - F)^+$; FAB-MS obsd 871.9958, calcd 871.9946; λ_{abs} 421, 553 nm; λ_{em} (λ_{ex} = 421 nm) 585, 641 nm.

5-Bromo-10,15,20-tris(pentafluorophenyl)porphinatozinc(II)-*1,9-*^{13}*C* (ZnP3-F$_{15}$(1,9-^{13}C)). Following a general procedure,[31] a solution of **ZnP2** (21 mg, 0.024 mmol) in dry $CHCl_3$ (4.8 mL, 5.0 mM) was treated with NBS (0.0240 mmol, 117 μL stock solution in dry $CHCl_3$, 0.205 M) and anhydrous pyridine (7 μL, 0.08 mmol) at 0 °C. The reaction was monitored by TLC and LD-MS. After 30 min the reaction was quenched by the addition of acetone. The solvent was evaporated. Column chromatography [silica, hexanes/CH_2Cl_2 (1:2)] gave a red-purple solid (19 mg, 85%): ^{1}H NMR δ 8.91−8.97 (m, 6H), 9.87−9.91 (m, 2H); ^{13}C NMR δ 131.6, 132.1, 132.39, 132.42, 150.5 (enh); LD-MS obsd 951.2; FAB-MS obsd 949.9084, calcd 949.9051 ($C_{36}{}^{13}C_2H_8BrF_{15}N_4Zn$); λ_{abs} 425, 551 nm; λ_{em} (λ_{ex} = 425 nm) 597, 648 nm; SEC t_R = 26.7 min (three-column series).

5-[4-[2-(4-Bromophenyl)ethynyl]phenyl]-10,15,20-tris(pentafluorophenyl)porphinatozinc(II) (ZnP4-F$_{15}$). Following a reported procedure,[29] reduction of tin complex **5** (204 mg, 0.219 mmol) in THF/MeOH (9 mL, 3:1) with $NaBH_4$ (324 mg, 8.76 mmol) afforded a yellow solid after the standard workup. The latter was then treated with **7** (87.0 mg, 0.219 mmol) in CH_2Cl_2 (88 mL, 2.5 mM) containing $Yb(OTf)_3$ (170 mg, 0.287 mmol) at room temperature. After 1.5 h, DDQ (149 mg, 0.657 mmol) was added to the reaction mixture. After 30 min, the reaction mixture was neutralized with TEA (200 μL). The crude reaction mixture was passed through a silica pad. The resulting purple solid was dissolved in $CHCl_3$ (9 mL) and treated overnight with $Zn(OAc)_2 \cdot 2H_2O$ (50.0 mg, 0.219 mmol) and MeOH (2 mL) at room temperature. Column chromatography (silica, CH_2Cl_2) gave a purple solid (55 mg, 22%): ^{1}H NMR δ 7.53−7.59 (m, 4H), 7.96 (d, J = 8.3 Hz, 2H), 8.22 (d, J = 8.3 Hz, 2H), 8.92−8.94 (m, 2H), 8.98−9.01 (m, 4H), 9.07−9.09 (m, 2H); ^{13}C NMR δ 90.0, 90.4, 104.1, 116.7, 122.3, 123.07, 123.11, 123.23, 130.3, 130.9, 131.8, 132.0, 132.2, 133.4, 134.3, 134.7, 136.4, 138.9, 142.2, 143.4, 145.5, 148.0, 149.9, 150.2, 150.5, 150.9; LD-MS obsd 1126.6; FAB-MS obsd 1123.9594, calcd 1123.9610 ($C_{52}H_{16}BrF_{15}N_4Zn$); λ_{abs} 422, 554 nm; λ_{em} (λ_{ex} = 422 nm) 588, 644 nm.

5-[4-[2-[4-(4,4,5,5-Tetramethyl-1,3,2-dioxaborolan-2-yl)phenyl]ethynyl]phenyl]-10,15,20-tris(pentafluorophenyl)porphinatozinc(II) (ZnP5-F$_{15}$). Following a reported procedure[34] with modification, samples of **ZnP4-F$_{15}$** (40 mg, 0.035 mmol), bis(pinacolato)diboron (71 mg, 0.28 mmol), and $PdCl_2(PPh_3)_2$ (3 mg, 0.002 mmol) were weighed into a 10 mL Schlenk flask which was then pump-purged three times with argon. Anhydrous, degassed 1,2-dichloroethane (3.8 mL, 10 mM) and TEA (12 equiv, 60 μL, 0.42 mmol) were added to the Schlenk flask. The resulting mixture was stirred at 75 °C for 40 h under argon. Column chromatography [silica, hexanes/CH_2Cl_2 (1:3)] afforded a pink-purple solid (25 mg, 60%): ^{1}H NMR δ 1.23 (s, 12H), 7.68 (d, J = 8.3 Hz, 2H), 7.88 (d, J = 8.3 Hz, 2H), 7.96 (d, J = 8.3 Hz, 2H), 7.21 (d, J = 8.3 Hz, 2H), 8.91−8.93 (m, 2H), 8.95−8.99 (m, 4H), 9.06−9.08 (m, 2H); LD-MS obsd 1172.9; FAB-MS obsd 1172.1356, calcd 1172.1357 ($C_{58}H_{28}BF_{15}N_4O_2Zn$); λ_{abs} 424, 548 nm; λ_{em} (λ_{ex} = 424 nm) 592, 646 nm; SEC t_R = 25.1 min (three-column series).

5,10,15-Tris(pentafluorophenyl)porphinatozinc(II)-*1,9-*^{13}*C-2,3,7,8,12,13,17,18,20-d*$_9$ (ZnP2-F$_{15}$(1,9-^{13}C)d$_9$). A sample of **ZnP2-F$_{15}$(1,9-^{13}C)** (15 mg, 0.017 mmol) was treated with D_2SO_4 (0.40 mL, 0.02 M) and stirred at 110 °C for 48 h. The reaction mixture was cooled to room temperature, and treated with saturated aqueous $NaHCO_3$ and CH_2Cl_2. The organic layer was separated, dried (K_2CO_3) and concentrated to give the free base porphyrin. The resulting product was dissolved in $CHCl_3$ (1 mL) and treated overnight with methanolic $Zn(OAc)_2 \cdot 2H_2O$ (5 mg, 0.02 mmol, 0.200 mL of MeOH) at room temperature. Column chromatography [silica, hexanes/CH_2Cl_2 (1:2)] afforded a bright-pink solid (10 mg, 67% yield, 95% isotopic purity): ^{1}H NMR δ 9.01−9.07 (weak signals), 9.52−9.56 (weak signals); ^{13}C NMR δ 150.11−150.18 (m, enh); LD-MS obsd 880.9, calcd 881.0511 ($C_{36}{}^{13}C_2D_9F_{15}N_4Zn$); λ_{abs} 416, 542, 576 nm; λ_{em} (λ_{ex} = 416 nm) 580, 636 nm. The ESI-MS data for the title compound were not satisfactory; however, data were satisfactory for the free base analogue (**P2-F$_{15}$(1,9-^{13}C)d$_9$**) obtained as an intermediate and used in the metalation described here: ESI-MS obsd 820.1446, calcd 820.1448 [$(M + H)^+$, $M = C_{36}{}^{13}C_2H_2D_9F_{15}N_4$].

***meso*-Tetrakis(pentafluorophenyl)porphyrin-*2,3,7,8,12,13,17,18-d*$_8$ (P6-F$_{20}$d$_8$).** A sample of **P6-F$_{20}$** (11 mg, 0.011 mmol) was treated with D_2SO_4 (1 mL) and stirred at 150 °C for 22 h. The LD-MS spectrum of the crude reaction mixture exhibited one peak (m/z = 983.9) corresponding to the fully deuteriated porphyrin containing 10 deuterons (β-pyrrole sites and the two inner pyrrolic nitrogens); calcd 984.1214 ($C_{44}D_{10}F_{20}N_4$). Neutralization of the reaction mixture with saturated aqueous $NaHCO_3$ and washing with H_2O resulted in proton/deuterium exchange at the inner nitrogen atoms. The product was isolated as a purple solid (10 mg, 92% yield, 97% isotopic purity): ^{1}H NMR δ −2.93 (s, 2H), 8.92 (s, 0.2H); LD-MS obsd 982.4; ESI-MS obsd 983.1160, calcd 983.1161 [$(M + H)^+$; $M = C_{44}H_2D_8F_{20}N_4$]; λ_{abs} 417, 508, 585, 641 nm; λ_{em} (λ_{ex} = 416 nm) 643, 713 nm.

***meso*-Tetrakis(pentafluorophenyl)porphinatozinc(II)-*2,3,7,8,12,13,17,18-d*$_8$ (ZnP6-F$_{20}$d$_8$).** Following a general procedure,[29] a solution of **P6-F$_{20}$d$_8$** (8 mg, 0.008 mmol) in $CHCl_3$ (1.6 mL) was treated with a solution of $Zn(OAc)_2 \cdot 2H_2O$ (9 mg, 0.04 mmol) in methanol (0.3 mL) at room temperature for 40 h. The reaction mixture was washed with water, dried (Na_2SO_4) and concentrated to dryness. Purification by column chromatography [silica, CH_2Cl_2/hexanes (2:1)] afforded a bright-pink solid (8 mg, quantitative yield, 97% isotopic purity): ^{1}H NMR δ 9.0 (s, weak signal); LD-MS obsd 1043.8; FAB-MS obsd 1044.0205, calcd 1044.0215 ($C_{44}D_8F_{20}N_4Zn$); λ_{abs} 421, 546 nm; λ_{em} (λ_{ex} = 421 nm) 586, 640 nm.

Zn$_2$D-F$_{30}$(1,9-^{13}C). Following a reported procedure,[20] samples of **ZnP3-F$_{15}$(1,9-^{13}C)** (10 mg, 0.010 mmol), **ZnP5-F$_{15}$** (12 mg, 0.010 mmol), $Pd(PPh_3)_4$ (4 mg, 0.003 mmol), and anhydrous K_2CO_3 (6 mg, 0.04 mmol; dried overnight at 150 °C in the high vacuum oven) were weighed into a 5 mL Schlenk flask which was then pump-purged three times with argon. Toluene/DMF [1 mL (2:1)] was added (the solvents were purged with argon for 30 min) and the reaction mixture was stirred at 90 °C under argon. After 27 h, analytical SEC indicated the presence of the product as the major component, traces of starting material, and some trimer material. Column chromatography (silica, CH_2Cl_2) removed the unreacted porphyrin monomers. The fraction containing the dyad was concentrated and then further purified by preparative SEC (toluene). A final adsorption chromatography column (silica, CH_2Cl_2) afforded a purple solid (9 mg, 50%): ^{1}H NMR δ 8.13 (d, J = 8.0 Hz, 4H), 8.32 (d, J = 7.6 Hz, 4H), 8.95−9.02 (m, 12H), 9.15−9.17 (m, 4H); ^{13}C NMR δ 150.2 (enh); LD-MS obsd 1916.5, calcd 1916.03 ($C_{88}{}^{13}C_2H_{24}F_{30}N_8Zn_2$); λ_{abs} 427, 553 nm; λ_{em} (λ_{ex} = 427 nm) 598, 650 nm; SEC t_r = 23.7 min (three-column series).

Zn$_2$D-F$_{30}$(1,9-^{13}C)d$_{24}$. A sample of **Zn$_2$D-F$_{30}$(1,9-^{13}C)** (5 mg, 0.002 mmol) was treated with D_2SO_4 (0.340 mL, 7.6 mM) and stirred at room temperature. The reaction was monitored by LD-MS. After 7 h, the reaction mixture was treated with saturated aqueous $NaHCO_3$ and CH_2Cl_2. The organic layer was separated, dried (K_2CO_3) and the solvent was evaporated to give a purple solid. The resulting free base porphyrin dyad was examined by ^{1}H NMR spectroscopy; comparison of the signals from the inner NH protons versus residual protons of the porphyrin β-pyrrole positions gave an estimate of 95% deuteriation. The free base porphyrin dyad was

dissolved in $CHCl_3$ (0.750 mL) and treated overnight with methanolic $Zn(OAc)_2 \cdot 2H_2O$ (5 mg, 0.02 mmol) and stirred at room temperature for 48 h. Column chromatography [silica, hexanes/CH_2Cl_2 (1:2) afforded a bright-pink solid (4 mg, 80% yield): ^1H NMR δ 8.12−8.14 (m, weak signals), 8.31−8.33 (m, weak signals), 8.98−8.99 (m, weak signals), 9.14−9.16 (m, weak signals); ^{13}C NMR δ 150.16−150.22 (m, enh), LD-MS obsd 1939.2, calcd 1940.18 ($C_{88}{}^{13}C_2D_{24}F_{30}N_8Zn_2$); λ_{abs} 424, 547 nm; λ_{em} (λ_{ex} = 424 nm) 587, 642 nm; SEC t_r = 41.7 min (five-column series).

Acknowledgment. This research was supported by grants from the Chemical Sciences, Geosciences and Biosciences Division, Office of Basic Energy Sciences, Office of Science, U.S. Department of Energy to D.H. (DE-FG02-05ER15661), J.S.L. (DE-FG02-96ER14632), and D.F.B. (DE-FG02-05ER15660). Mass spectra were obtained at the Mass Spectrometry Laboratory for Biotechnology at North Carolina State University. Partial funding for the NCSU Facility was obtained from the North Carolina Biotechnology Center and the NSF.

Supporting Information Available: General procedures and spectral data for new compounds. This material is available free of charge via the Internet at http://pubs.acs.org.

JO8012836